Records of Natural Products

www.acgpubs.org
ORIGINAL ARTICLE

Hengshanols F and G, two new acylphloroglucinols from *Hypericum hengshanense*

Siyi Liao[1#], Qindi Han[1#], Wenqing Huang[1], Cong Jing[1], Xiuteng Zhou[2], Alibek Ydyrys[3], Qinxiong Lin[1*] and Xinzhou Yang[1*]

[1]School of Pharmaceutical Sciences, South-Central Minzu University, Wuhan 430074, China
[2]State Key Laboratory of Dao-di Herbs, National Resource Center for Chinese Materia Medica, China Academy of Chinese Medical Sciences, Beijing 100700, China
[3]Biomedical Research Centre, Al-Farabi Kazakh National University, 71 Al-Farabi Avenue, 050040, Kazakhstan

Abstract: Two new acylphloroglucinols, hengshanols F and G (**1** and **2**), were isolated from *Hypericum hengshanense*, together with nine known phloroglucinol derivatives: dauphinol F (**3**), 4-geranyl-2-(2′-methylpropionyl)-phloroglucinol (**4**), 1-[5,7-dihydroxy-2-methyl-2-(4-methylpent-3-enyl)-chroman-8-yl]-2-methylpropan-1-one (**5**), 1-[5,7-dihydroxy-2-methyl-2-(4-methylpent-3-enyl)-chroman-8-yl]-2-methylbutan-1-one (**6**), empetriferdinan B (**7**), tomoeone B (**8**), uraloidin A (**9**), hyperbeanol P (**10**), ascyronone G (**11**). The structures of the two new acylphloroglucinols were determined by 1D NMR (^{1}H, ^{13}C, DEPT), 2D NMR (HMBC, COSY, HSQC), HRMS and electronic circular dichroism (ECD). The structural elucidation revealed that all isolated compounds (**1**–**11**) are phloroglucinol derivatives. In cell viability assays, compounds **1**, **5**, **8**, and **9** significantly reduced cell viability. whereas compound **6** promoted ATP production and enhanced mitochondrial activity.

Keywords: *Hypericaceae*, *Hypericum hengshanense*, phloroglucinol derivative, cell viability assay

Cite this article as:
Liao et al. Hengshanols F and G, two new acylphloroglucinols from *Hypericum hengshanense*. (2026). *Records of Natural Products*, 20(6):e26023748

Received: *13 February 2026*
Revised: *01 June 2026*
Accepted: *03 June 2026*
Published: *11 June 2026*

1 Introduction

The family Guttiferae, also known as Clusiaceae, is a group of dicotyledonous plants primarily distributed in tropical regions. It comprises approximately 40 genera and over 1,000 species, classified into five subfamilies (Xu et al., 2017). The genus Hypericum belongs to one of these subfamilies and is widely distributed throughout China, with the greatest diversity found in the southwestern region (Song et al., 2021).

In traditional Chinese medicine, plants of the genus *Hypericum* are believed to have functions such as clearing heat, detoxifying, promoting hemostasis, and eliminating dampness. They are commonly used to alleviate symptoms including hemoptysis, hematemesis, intestinal hemorrhage, traumatic bleeding, rheumatic pain, and oral or nasal sores (Yin et al., 2013). Recent studies have expanded their pharmacological profile to include antidepressant, antitumor, antiviral, analgesic, antibacterial, and anti-inflammatory activities (Nahrstedt & Butterweck, 1997; Xiao & Mu, 2007). Notably, phloroglucinol derivatives, primarily isolated from *Hypericum* species, exhibit antitumor, antibacterial, and antidepressant effects, making them important natural products and promising candidates for drug development (Zhao et al., 2021).

Hypericum hengshanense W. T. Wang, a member of the genus *Hypericum*, is mainly found in western Jiangxi (Yongxin) and eastern Hunan (Hengshan). This species typically grows on slopes, along roadsides, or under shrubs at elevations of around 820 m. In traditional Chinese medicine, the entire plant is often used to alleviate inflammation, hepatitis, and swelling or pain (Wang & Xu, 2013). Its traditional use may be associated with the modulation of cellular energy metabolism and function—a connection supported by the established role of mitochondria as the cell's energy center and their involvement in diseases such as tumors and metabolic disorders (Zong et al., 2016; Crouch et al., 1993). The present study focuses on adenosine triphosphate (ATP), a critical marker of cellular energy status. Intracellular ATP levels were measured using the CellTiter-Lite luminescent assay to assess the effects of the isolated compounds on cell viability (Riss & Moravec, 2004). To further explore potential cytotoxic effects, DAPI staining was performed to examine nuclear morphology and cell count.

*Corresponding Authors: Qinxiong Lin. Email: clyhappy05@163.com; Xinzhou Yang. Email: xzyang@mail.scuec.edu.cn
[#]These authors (Siyi Liao[#], Qindi Han[#]) contributed equally to this work.

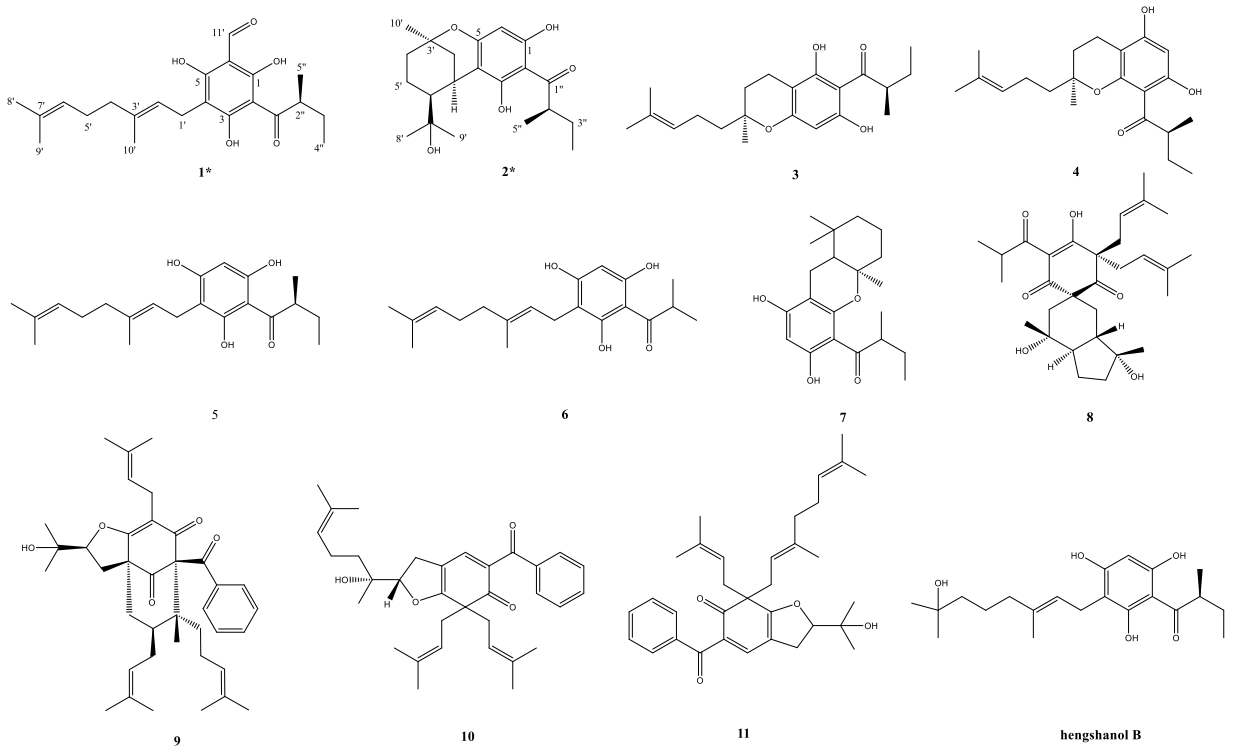

Figure 1. Chemical structures of compounds **1**–**11** isolated from *Hypericum hengshanense*

2 Experimental Section

2.1 Instruments and Materials

NMR spectra were recorded using a Bruker Ascend III™ 600 MHz spectrometer (Bruker, Fallanden, Switzerland). UV–Vis spectra were measured with a Shimadzu UV-250 spectrophotometer (Shimadzu, Tokyo, Japan), and IR spectra were obtained using a Shimadzu FTIR-8400S spectrometer (Shimadzu, Kyoto, Japan). Optical rotations were determined with an Autopol IV-T automatic polarimeter (Rudolph Research Analytical, USA). LC–MS analysis was performed on a Waters ACQUITY SQD MS system (Waters, USA), and CD spectra were recorded with a JASCO J-720W circular dichroism spectrometer (JASCO, Tokyo, Japan). For column chromatography, silica gel (300–400 mesh) and silica gel GF254 plates were purchased from Yantai Jiangyou (Yantai, China). HPLC purification was performed on a Waters 2535 system (Waters, USA) equipped with a 2998 photodiode array detector and a 2707 autosampler, using C18, PFP, and Chloster columns (5 μM, 10 × 250 mm; COSMOSIL, Kyoto, Japan).

2.2 Plant Material

Specimens of *Hypericum hengshanense* W. T. Wang were collected in Hengyang City, Hu nan Province, in July 2019. The species was identified by Prof. Wan Dingrong (School of Pharmaceutical Sciences, South-Central Minzu University). A voucher specimen (No. SC0866) has been deposited in the herbarium of the same institution. As this herbarium is not registered in the Index Herbariorum, the specimen is referenced by its internal accession number.

2.3 Isolation and Purification

The dried aerial parts of *Hypericum hengshanense* (9.4 kg) were ground into powder, and the powdered material was soaked in 80% ethanol. The extract was then concentrated under reduced pressure using a rotary evaporator to yield 1.84 kg of crude ethanol extract. This crude extract was suspended in hot distilled water (2.0 L) and then sequentially extracted with petroleum ether, ethyl acetate, and n-butanol. After concentration under reduced pressure, three fractions were obtained: petroleum ether (156 g), ethyl acetate (841 g), and butanol (295 g). Because the petroleum ether fraction was relatively small, it was combined with the ethyl acetate fraction to give a combined fraction of 997 g, of which 950 g was subjected to further separation. The combined fractio n was initially separated by HP20 macroporous resin column chromatography using a water–ethanol gradient. Based on TLC analysis, twelve subfractions (Fr. 1–Fr. 12) were collected.

Fr.7 (300 g) was separated by normal-phase silica gel column chromatography, with silica gel filler of 300–400 mesh, using a dichloromethane–methanol gradient, yielding seven fractions (Fr. 7.1–Fr. 7.7) as determined by TLC analysis.

Compound **6** was isolated from Fr. 7.1.1, compound **3** from Fr. 7.3.5, and compounds **8** and **9** from Fr. 7.6.4. Fr. 7.6.1 yielded new compounds **1** and **2**, along with known compounds **7**, **10**, and **11**. Compounds **4** and **5** were isolated from Fr. 7.9.1 and Fr. 7.9.12, respectively. All of these compounds

https://doi.org/10.25135/rnp.2602.3748
Rec. Nat. Prod. 2026, 20(6):e26023748

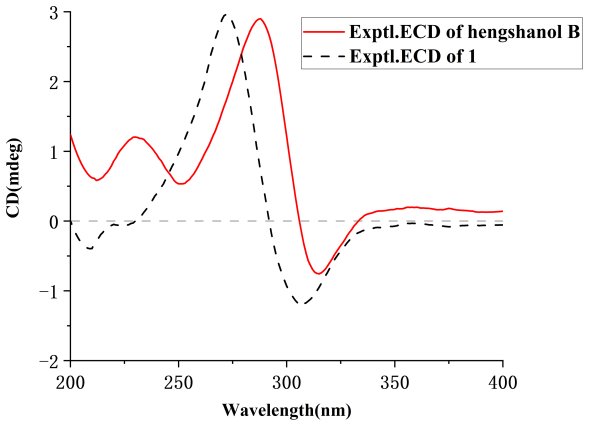

Figure 2. The CD spectrum of compound **1**

were purified by sequential chromatography on Sephadex LH-20 and HPLC.

3 Results and Discussion

3.1 Structural Features and Identification

Compound **1** is a yellow oil. HR-ESI-MS data established its molecular formula as $C_{22}H_{30}O_5$ (*m/z* 375.2167 $[M + H]^+$, calcd 375.2166), indicating eight degrees of unsaturation. The IR spectrum showed characteristic absorption bands at 3406 cm^{-1} (hydroxy group), 1673 cm^{-1} (conjugated carbonyl group), and 1620 cm^{-1} (aromatic ring), as well as aliphatic C–H stretches in the 2850–2960 cm^{-1} region. The ^1H NMR spectrum of **1** showed five methyl signals [δ_H 1.82 (3H, s, H-10′), 1.68 (3H, s, H-8′), 1.61 (3H, s, H-9′), 1.17 (3H, m, H-5″), 0.93 (3H, m, H-4″)], two olefinic protons [δ_H 5.30 (1H, m, H-2′), 5.03 (1H, m, H-6′)], and four methylene groups [δ_H 3.39 (2H, m, H-1′), 2.14 (2H, m, H-4′), 2.14 (2H, m, H-5′), 1.85 (1H, m, H-3″), 1.41 (1H, m, H-3″)]. The ^{13}C NMR and DEPT spectra revealed 21 carbon resonances, consisting of five methyls, four methylenes, nine quaternary carbons (including one oxygenated carbonyl, six aromatic carbons, and two olefinic carbons), and three tertiary carbons (one aldehyde and two olefinic carbons). Comparison of the ^1H and ^{13}C chemical shifts and coupling constants revealed that compound **1** shares a high degree of structural similarity with the known monocyclic phloroglucinol derivative **5** (1-[5,7-dihydroxy-2-methyl-2-(4-methylpent-3-enyl)-chroman-8-yl]-2-methylpropan-1-one) (Winkelmann et al., 2003), indicating that both compounds belong to the same class of phloroglucinol derivatives. The main difference was that the aromatic proton at δ_H 7.74 (d, J = 8.8 Hz) in **5** was replaced in **1** by an aldehyde proton at δ_H 10.04 (s, H-11′) and a corresponding carbonyl carbon at δ_C 192.2 (C-11), suggesting the introduction of a formyl group at the C-6 position. This was confirmed by an HSQC correlation between H-11′ and C-11, together with HMBC cross-peaks from H-11′ to C-6 (δ_C 103.7), C-5 (δ_C 168.1), and C-11 (δ_C 192.2), which established the attachment of the aldehyde group to C-6 of the aromatic ring. Compound **1** exhibited a negative Cotton effect at 288 nM and a positive Cotton effect at 313 nM

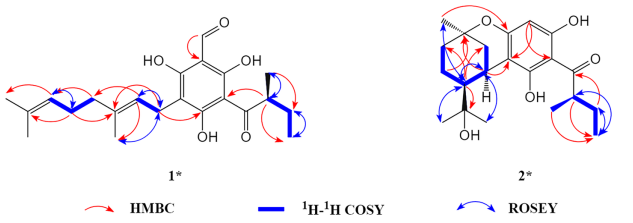

Figure 3. The key HMBC, ^1H-^1H COSY and ROESY correlations of compounds **1** and **2**

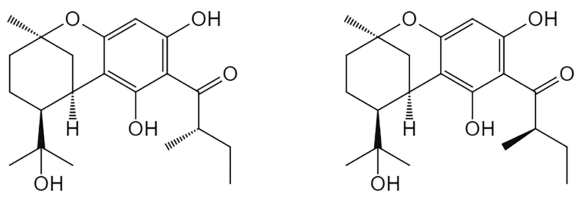

Figure 4. Predicted chemical structures for the two candidate stereoisomers of compound **2**: (1′R*, 3′R*, 6′S*, 2″S*)-**2** and (1′R*, 3′R*, 6′S*, 2″R*)-**2**

in its CD spectrum. Its ECD profile was nearly identical to that of the known compound hengshanol B (Han et al., 2022) (Figure 2), with consistent chiral carbon configurations. Accordingly, the absolute configuration at C-2″ was assigned as S, and compound **1** was named hengshanol F.

Compound **2** is a yellow oil. HR-ESI-MS data established its molecular formula as $C_{21}H_{30}O_5$ (*m/z* 363.2165 $[M + H]^+$, calcd 363.2166), indicating eight degrees of unsaturation. The IR spectrum showed characteristic absorption bands at 3406 cm^{-1} (O–H stretching), 2937 cm^{-1} (C–H stretching), 1573 and 1489 cm^{-1} (aromatic C=C stretching), 1361 cm^{-1} (C–H bending), and 1203, 1157, and 1010 cm^{-1} (C–O stretching), along with additional absorptions in the fingerprint region. The ^1H NMR spectrum of **2** showed five methyl signals [δ_H 1.34 (3H, s, H-10′), 1.18 (3H, s, H-8′), 1.12 (3H, s, H-5″), 0.91 (3H, s, H-9′), 0.88 (3H, s, H-4″)], two methylene signals [δ_H 3.91 (1H, m, H-2″), 3.44 (1H, d, H-1′)], four methylene groups [δH 1.97 (1H, m, H-4′), 1.92 (1H, m, H-2a′), 1.82 (1H, m, H-3″), 1.67 (1H, m, H-2b′), 1.61 (1H, m, H-4′), 1.53 (1H, m, H-5′), 1.37 (1H, m, H-3″), 1.24 (1H, m, H-5′)], and one isolated aromatic/olefinic proton [δ_H 5.84 (1H, s, H-6)]. The ^{13}C NMR and DEPT spectra of **2** revealed 21 carbon resonances, consisting of six aromatic carbons, one carbonyl carbon, two oxygenated tertiary carbons, three methines, four methylenes, and five methyl carbons. Comparison of the NMR data with literature values indicated that compound **2** closely resembled the known acylphloroglucinol-based meroterpenoid (±)-Japonicol A (Hu et al., 2016). The main structural difference lies in the replacement of a methyl signal at δ_H 1.09 (3H, s, H-9″) in (±)-Japonicol A with two methylene signals at δ_H 1.82 and 1.37 (each 1H, m, H-4″) in 2, and the hydroxy signal at δ_H 5.02 (1H, d, J = 4.0 Hz, 2-OH) in the known compound was replaced by two methylene signals at δ_H 1.92 and 1.67 (each 1H, m, H-2″)

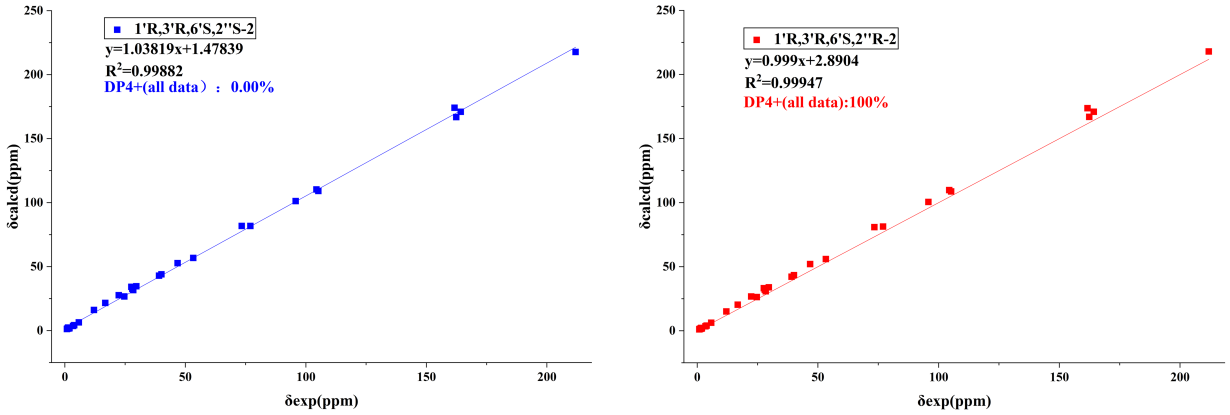

Figure 5. Linear correlation of experimental versus calculated ^{13}C NMR and ^{1}H NMR chemical shifts for the two candidate configurations (1′R*, 3′R*, 6′S*, 2″S*)-**2** and (1′R*, 3′R*, 6′S*, 2″R*)-**2** of compound **2**

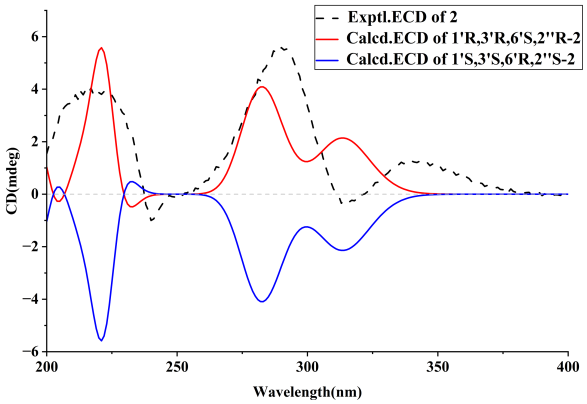

Figure 6. Experimental and calculated ECD spectra of compound **2**

in **2**. These modifications were supported by HMBC and ^{1}H-^{1}H COSY correlations. Specifically, HMBC cross-peaks were observed between H-3″ (δ_H 3.91 and 1.37) and H-4″ (δ_H 0.88), while COSY correlations were detected between H-2″ (δ_H 1.92 and 1.67) and H-1″ (δ_H 3.44), as well as with δ_C 105.2 (C-4), δ_C 27.6 (C-1′), and δ_C 53.3 (C-6′) (Figure 3). The relative configuration of compound **2** was determined using ROESY analysis and computational NMR chemical shift predictions (Figure 1). Key ROESY correlations were observed for H-1′/H-6′, H-6/H-2b, and H-6′/Me-10. Since compound **2** possesses the same bicyclo[3.3.1]nonane skeleton as (±)-Japonicol A, the C-1′/C-4 and C-3′/O bonds were assigned as axial. Accordingly, the relative configurations at C-1′, C-3′, and C-6′ were deduced to be consistent with those of (±)-Japonicol A, leading to the assignment of 1′R, 3′R, 6′S*. Because the relative configuration at C-2″ could not be determined by ROESY, computational predictions of NMR chemical shifts were performed for two possible diastereomers, (1′R, 3′R, 6′S, 2″S)-**2** and (1′R, 3′R, 6′S, 2″R)-**2** (Figure 4), using the GIAO method at the mPW1PW91/6-311G (d, p) level with the PCM solvation model in methanol. The calculated data for (1′R, 3′R, 6′S, 2″R)-**2** (R^2 = 0.99947) showed better agreement with the experimental values than the other diastereomer (R^2 = 0.99882). This assignment was further supported by DP4+ probability analysis, which assigned a 100.00% probability to the (1′R, 3′R, 6′S, 2″R)-**2** configuration (Figure 5). TD-DFT calculations at the B3LYP/6-311+G (d, p) level using the PCM model in methanol generated the theoretical ECD spectrum for (1′R, 3′R, 6′S, 2″R)-**2**. The close match between this calculated spectrum and the experimental ECD profile of compound **2** (Figure 6) confirmed its absolute configuration. Based on the combined evidence, the complete structure of compound **2** was determined and designated as hengshanol G.

The nine known compounds were identified by comparing their spectroscopic and physicochemical data with previously reported values. These compounds include dauphinol F (**3**) (Fuentes et al., 2019), 4-geranyl-2-(2′-methyl propionyl)-phloroglucinol (**4**) (Fuentes et al., 2019), 1-[5,7-dihydroxy-2-methyl-2-(4-methylpent-3-enyl)-chroman-8-yl]-2-methylpropan-1-one (**5**) (Winkelmann et al., 2003), 1-[5,7-dihydroxy-2-methyl-2-(4-methylpent-3-enyl)-chroman-8-yl]-2-methylbutan-1-one (**6**) (Winkelmann et al., 2003), empetriferdinan B (**7**) (Schmidt et al., 2012), tomoeone B (**8**) (Hashida et al., 2008), uraloidin A (**9**) (Guo et al., 2008), hyperbeanol P (**10**) (Li et al., 2019), and ascyronone G (**11**) (Li et al., 2019) (Figure 1).

3.2 Cell Viability Assay

The effects of selected compounds on HepG2 cells were evaluated using the CellTiter-Lite luminescent assay (Crouch et al., 1993; Park et al., 2023; Shao et al., 2022). This method assesses cell viability by measuring intracellular ATP levels, thereby enabling evaluation of the compounds cytotoxic effects. As shown in Figure 7A, compounds **1** (0.92-fold), **5** (0.11-fold), **8** (0.81-fold), and **9** (0.10-fold) caused a significant decrease in cell viability (*p < 0.05 or ***p < 0.001). In contrast, compound **6** (1.06-fold, ***p < 0.001) significantly increased cell viability, suggesting a potential role in promoting ATP production and mitochondrial function. Consistent with these results, DAPI staining (Figure 7B) revealed a marked reduction in cell number after 36 hours of treatment with compounds **1**, **5**, **8**, and **9**, providing morphological

https://doi.org/10.25135/rnp.2602.3748
Rec. Nat. Prod. 2026, 20(6):e26023748

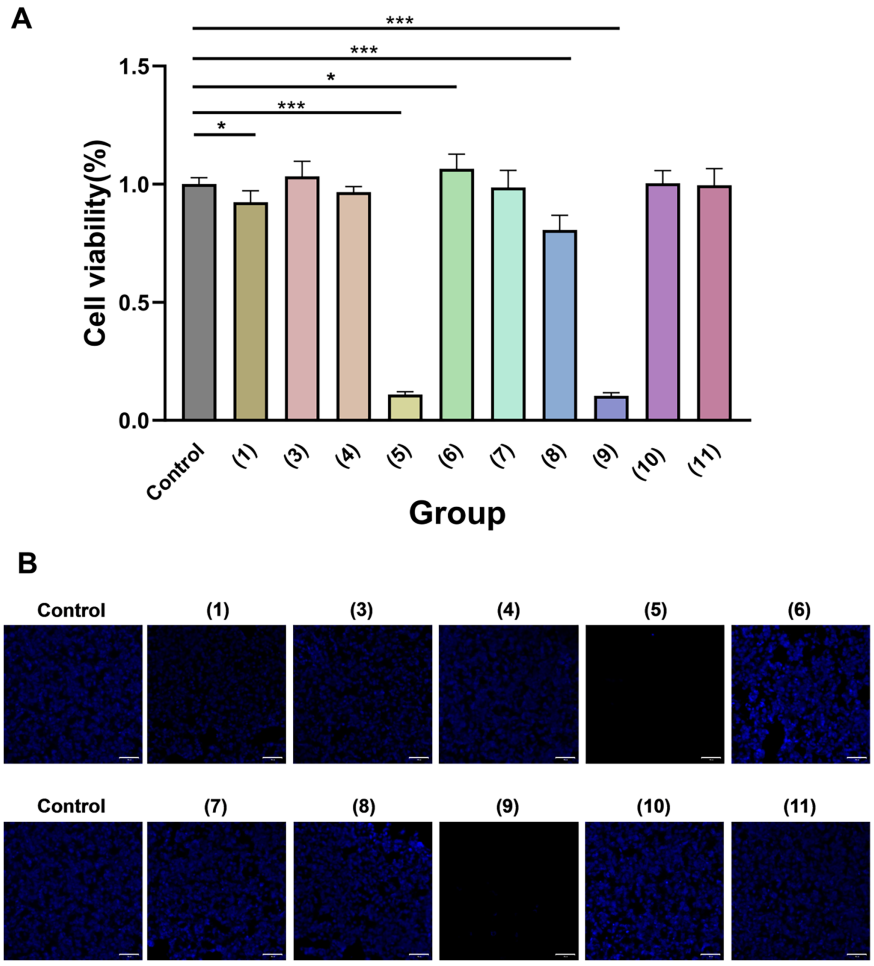

Figure 7. Effects of the tested compounds on HepG2 cells. (**A**) Cell viability following treatment with each compound (50 μg·mL^{-1}, n = 8). (**B**) Nuclear fluorescence intensity of HepG2 cells under the same conditions (n = 3). All data are expressed as mean ± SEM. Asterisks indicate statistically significant differences compared to the control group (*$p < 0.05$, **$p < 0.01$, ***$p < 0.001$).

evidence that supports the cell viability findings (Wang et al., 2023).

3.3 Conclusion

Two new acylphloroglucinols compounds (**1** and **2**), along with nine known compounds (**3**–**11**), were isolated from *Hypericum hengshanense*. Their structures were elucidated by spectroscopic analysis. In addition, the CellTiter-Lite luminescent cell viability assay revealed that compounds **1**, **5**, **8**, and **9** significantly reduced cell viability, suggesting potential antitumor effects. In contrast, compound **6** increased cell viability and enhanced cellular ATP production. Overall, this study enriches the chemical and pharmacological understanding of the *Hypericum* genus, providing new insights and a scientific basis for further research.

3.4 Characterization of Compounds

Hengshanol F (***1***): yellow oil; $[\alpha]^{20}_{D}$ +9.6 (*c* 0.50, MeOH). UV (MeOH); λ_{max} (log ε): 265 (3.644), 275 (3.600). IR ν_{max} (cm^{-1}): 2970, 2931, 2877, 1620, 1435, 1381, 1300, 1184, 601. ^{1}H and ^{13}C NMR spectroscopic data can be found in Table 1. HR-ESI-MS *m/z* 375.2167 [M + H]$^{+}$ (calcd for 375.2166).

Hengshanol G (***2***): yellow oil; $[\alpha]^{20}_{D}$ +43.8 (*c* 0.50, MeOH). UV (MeOH); λ_{max} (log ε): 218 (3.122), 290 (3.528). IR ν_{max} (cm^{-1}): 3406, 2974, 2935, 2873, 1620, 1573, 1489, 1411, 1361, 1203, 1157, 1010, 914, 891, 825, 763. ^{1}H and ^{13}C NMR spectroscopic data can be found in Table 1. HR-ESI-MS *m/z* 363.2165 [M + H]$^{+}$ (calcd for 363.2166).

The ^{1}H and ^{13}C NMR chemical shifts for the remaining nine known compounds are provided in the Supporting Information.

Table 1. ^{1}H NMR (600 MHz) and ^{13}C NMR (125 MHz) data for Compounds **1** and **2**

Position	1 (in $CDCl_3$)		2 (in CD_3OD)	
	δ_H	δ_H	δ_H	δ_H
1	–	164.1	–	161.7
2	–	104.0	–	104.4
3	–	171.9	–	162.9
4	–	104.5	–	105.2
5	–	168.1	–	164.3
6	–	103.7	5.84, s	95.8
1′	3.39, d, (7.3)	21.4	3.44, d, (3.1)	27.6
2′a 2′b	5.30, t, (7.3)	121.1	1.67, m 1.92, dd, (9.9, 3.3)	39.1
3′	–	142.1	–	77.0
4′	2.14, d, (4.7)	39.8	1.61, td, (13.5, 4.8) 1.97, m	40.1
5′	2.14, d, (4.7)	26.1	1.24, ddd, (13.4 4.3 1.7) 1.53, d, (13.0)	22.4
6′	5.03, m	123.4	1.79, m	53.3
7′	–	132.9	–	73.4
8′	1.68, s	25.9	1.18, s	29.7
9′	1.61, s	17.8	0.91, s	24.7
10′	1.82, s	16.5	1.34, s	28.4
11′	10.04, s	192.2	–	–
1″	–	211.3	–	211.9
2″	3.81, sext, (6.7)	46.2	3.91, sext, (6.7)	46.5
3″	1.41, dp, (14.6, 7.3) 1.85, s	26.9	1.37, m 1.82, m	28.0
4″	0.93, t, (7.4)	12.1	0.88, m	12.1
5″	1.17, d, (6.9)	16.3	1.12, d, (6.8)	16.8

Funding Statement

This study was supported financially by This work is funded by the Natural Science Foundation of China grant (82374144), the Fundamental Research Funds for the Central Universities, South-Central Minzu University (CZD24003, XTZ24026).

Author Contributions

Si-Yi Liao: Data curation and Writing–original draft; Qing-Di Han: Data curation; Wen-Qing Huang: Data curation; Cong Jing: Methodology, Data curation; Xiu-Teng Zhou: Methodology, Analysis, Investigation; Alibek ydyrys: Methodology, Analysis, Investigation; Qin-Xiong Lin: Writing-review & editing, Funding, and Supervision; Xin-Zhou Yang: Writing-review & editing, Funding, and Supervision.

Availability of Data and Materials

The authors declare that the data supporting the findings of this study are available within the paper and its Supplementary Information files. Should any raw data files be needed in another format they are available from the corresponding author upon reasonable request. Source data are provided with this paper.

Conflicts of Interest

The authors declare that they do not have any conflict of interest.

Supporting Information

Supporting information accompanies this paper on http://www.acgpubs.org/journals/records-of-natural-products.

ORCID

Siyi Liao: 0009-0000-7441-4677
Qindi Han: 0009-0007-9461-3076
Wenqing Huang: 0009-0005-0843-6903
Cong Jing: 0009-0001-4669-8796
Xiuteng Zhou: 0000-0002-9012-794X

Alibek Ydyrys: 0000-0002-5561-0856
Qinxiong Lin: 0009-0004-9918-6040
Xinzhou Yang: 0000-0003-1697-2923

References

Crouch, S. P., Kozlowski, R., Slater, K. J. & Fletcher, J. (1993). The use of ATP bioluminescence as a measure of cell proliferation and cytotoxicity. *Journal of Immunological Methods*, *160*, 81–88. DOI: 10.1016/0022-1759(93)90011-u.

Fuentes, R. G., Pearce, K. C., Du, Y., Rakotondrafara, A., Valenciano, A. L., Cassera, M. B., Rasamison, V. E., Crawford, T. D. & Kingston, D. G. I. (2019). Phloroglucinols from the roots of *Garcinia dauphinensis* and their antiproliferative and antiplasmodial activities. *Journal of Natural Products*, *82*, 431–439. DOI: 10.1021/acs.jnatprod.8b00379.

Guo, N., Chen, X. Q. & Zhao, Q. S. (2008). A new Polyisoprenylated Benzoylphloroglucinol derivative from *Hypericum henryi* subsp.uraloides (Guttiferae). *Journal of Yunnan Botanical Research*, *30*, 515–518. DOI: 10.3969/j.issn.2095-0845.2008.04.021.

Han, Q., Shu, G., Cheng, H., Wang, S., Zhou, T., Zhou, X., Sefidkon, F., Hossseini, M. M. Z., Kang, L. & Yang, X. (2022). New Aclyphloroglucinols and geranyl-α-pyrones from *Hypericum hengshanense*. *Fitoterapia*, *162*, 105253. DOI: 10.1016/j.fitote.2022.105253.

Hashida, W., Tanaka, N., Kashiwada, Y., Sekiya, M., Ikeshiro, Y. & Takaishi, Y. (2008). Tomoeones A-H, cytotoxic phloroglucinol derivatives from *Hypericum ascyron*. *Phytochemistry*, *69*, 2225–2230. DOI: 10.1016/j.phytochem.2008.04.026.

Hu, L., Xue, Y., Zhang, J., Zhu, H., Chen, C., Li, X. N., Liu, J., Wang, Z., Zhang, Y. & Zhang, Y. (2016). (±)-Japonicols A-D, Acylphloroglucinol-based meroterpenoid enantiomers with anti-KSHV activities from *Hypericum japonicum*. *Journal of Natural Products*, *79*, 1322–1328. DOI: 10.1021/acs.jnatprod.5b01119.

Li, Z. P., Kim, J. Y., Ban, Y. J. & Park, K. H. (2019). Human neutrophil elastase (HNE) inhibitory polyprenylated acylphloroglucinols from the flowers of *Hypericum ascyron*. *Bioorganic Chemistry*, *90*, 103075. DOI: 10.1016/j.bioorg.2019.103075.

Li, Y. R., Xu, W. J., Wei, S. S., Lu, W. J., Luo, J. & Kong, L. Y. (2019). Hyperbeanols F-Q, diverse monoterpenoid polyprenylated acylphloroglucinols from the flowers of *Hypericum beanii*. *Phytochemistry*, *159*, 56–64. DOI: 10.1016/j.phytochem.2018.12.005.

Nahrstedt, A. & Butterweck, V. (1997). Biologically active and other chemical constituents of the herb of *Hypericum perforatum L*. *Pharmacopsychiatry*, *30*, 129–134. DOI: 10.1055/s-2007-979533.

Park, J. S., Kim, Y. W., Kim, H., Kim, S. K. & Park, K. (2023). Development of a novel ATP bioluminescence assay based on engineered probiotic saccharomyces boulardii expressing firefly luciferase. *Journal of Microbiology and Biotechnology*, *33*, 1506–1512. DOI: 10.4014/jmb.2305.05019.

Riss, T. L. & Moravec, R. A. (2004). Use of multiple assay endpoints to investigate the effects of incubation time, dose of toxin, and plating density in cell-based cytotoxicity assays. *Assay and Drug Development Technologies*, *2*, 51–62. DOI: 10.1089/154065804322966315.

Schmidt, S., Jürgenliemk, G., Schmidt, T. J., Skaltsa, H. & Heilmann, J. (2012). Bi-, tri-, and polycyclic acylphloroglucinols from *Hypericum empetrifolium*. *Journal of Natural Products*, *75*, 1697–1705. DOI: 10.1021/np300237n.

Shao, S., Zhuang, X., Zhang, L. & Qiao, T. (2022). Antidepressants fluoxetine mediates endoplasmic reticulum stress and autophagy of non-small cell lung cancer cells through the ATF4-AKT-mTOR signaling pathway. *Frontiers in Pharmacology*, *13*, 904701. DOI: 10.3389/fphar.2022.904701.

Song, P., Hao, J., Wang, Y. & Yang, X. Z. (2021). Polycyclic polyprenylated acylphloroglucinols from Hypericum species and their biological activities. *China Journal of Chinese Materia Medica*, *46*, 4881–4890. DOI: 10.19540/j.cnki.cjcmm.20210603.601.

Wang, X., Tian, Y., Lin, H., Cao, X. & Zhang, Z. (2023). Curcumin induces apoptosis in human hepatocellular carcinoma cells by decreasing the expression of STAT3/VEGF/HIF-1α signaling. *Open Life Sciences*, *18*, 20220618. DOI: 10.1515/biol-2022-0618.

Wang, Q. & Xu, F. H. (2013). Chemical constituents of ethyl acetate fraction from *Hypericum hengshanense*. *Chinese Medicinal Materials*, *36*, 1611–1613. DOI: 10.13863/j.issn1001-4454.2013.10.023.

Winkelmann, K., San, M., Kypriotakis, Z., Skaltsa, H., Bosilij, B. & Heilmann, J. (2003). Antibacterial and cytotoxic activity of prenylated bicyclic acylphloroglucinol derivatives from *Hypericum amblycalyx*. *Zeitschrift für Naturforschung C*, *58*, 527–532. DOI: 10.1515/znc-2003-7-814.

Xiao, Z. Y. & Mu, Q. (2007). Advences on chemical investigation of hypericum. *Natural Product Research and Development*, *19*, 344–355. DOI: 10.3969/j.issn.1001-6880.2007.02.042.

Xu, S. C., Niu, S. L., Qin, W. Q., Huang, Z. C., An, H., Liu, Y. J., Wang, Y. & Liu, B. (2017). The ethnobotanical investigation of Clusiaceae plants in Chinese tropical area. *Anhui Agricultural Sciences*, *45*, 12–16. DOI: 10.13989/j.cnki.0517-6611.2017.09.004.

Yin, X. B., Jia, Y. J., Cao, S. L., Shen, M. R., Fu, J. & Ni, J. (2013). Advance of pharmacological studies on *Hypericum Perforatum*. *Clinical Journal of Traditional Chinese Medicine*, *31*, 1634–1637. DOI: 10.13193/j.issn.1673-7717.2013.08.072.

Zhao, X. B., Guo, Y., Wang, Y. Y. & Zhang, Y. H. (2021). Research progress of polycyclic polyprenylated acylphloroglucinols natural products. *China Journal of Chinese Materia Medica*, *46*, 3076–3086. DOI: 10.19540/j.cnki.cjcmm.20200329.601.

Zong, W. X., Rabinowitz, J. D. & White, E. (2016). Mitochondria and cancer. *Molecular Cell*, *61*, 667–676. DOI: 10.1016/j.molcel.2016.02.011.